5-2016

Peptoid morphology studies and its performance in inhibiting islet amyloid polypeptide

Dongwon Park

Peptoid morphology studies and its performance in inhibiting islet amyloid polypeptide

Dongwon Park

University of Arkansas, Fayetteville
May 2016

Table of Contents

1. Introduction

1.1 Misfolded proteins.....1

1.1.1 Alzheimer disease (Amyloid beta).....2

1.1.2 Type 2 diabetes (Amylin) 4

1.2 What is Peptoid ?.....5

2. Previous Research on Misfolded proteins

2.1 Chaperones.....6

2.2 Gold nanoparticles.....7

2.3 Peptoides.....8

3. Modulating Amyloid-β Aggregation: The Effects of Peptoid Side Chain Placement and Chirality

3.1 Aim of Research.....9

3.2 Research methods.....10

3.3 Results & Discussions.....12

3.4 Conclusion.....16

4. Amyloid Beta Peptoid Inhibitor Prevents fibril Formation of Islet Amyloid Polypeptide

4.1 Aim of Research.....17

4.2 Research methods.....18

4.3 Results & Discussions.....19

4.4 Conclusion.....23

A. APPENDIX

A.1 List of References.....25

A.2 List of Abbreviations.....30

A.3 List of Figures.....31

1. Introduction

1.1 Misfolded Proteins

Proteins are large biomolecules that consist of one or more chains of amino acids. They perform essential and diverse functions that are related to: hormone, enzyme, structural, immune, and storage [1]. The biological functions of each protein result from its amino sequence and its folding process, which determines its three-dimensional structure [2]. However, the protein folding process can be disrupted by failing to reach the active state [3]. When the proteins misfold, they display highly ordered structures that are insoluble in normal conditions [4, 5]. Aggregated proteins are believed to prompt pathological conditions in multiple organs, and the diseases are named as protein conformational disorders (PCD) [4, 6-8]. Table 1 lists diseases caused by misfolded proteins and their corresponding aggregate components.

Table 1 A summary of the main amyloidoses and the proteins or peptides involved

Disease	Main aggregate component
Alzheimer's disease	Aβ peptides (plaques); tau protein (tangles)
Spongiform encephalopathies	Prion (whole or fragments)
Parkinson's disease	α-synuclein (wt or mutant)
Primary systemic amyloidosis	Ig light chains (whole or fragments)
Secondary systemic amyloidosis	Serum amyloid A (whole or 76-residue fragment)
Fronto-temporal dementias	Tau (wt or mutant)
Senile systemic amyloidosis	Transthyretin (whole or fragments)
Familial amyloid polyneuropathy I	Transthyretin (over 45 mutants)
Hereditary cerebral amyloid angiopathy	Cystatin C (minus a 10-residue fragment)
Haemodialysis-related amyloidosis	β_2-microglobulin
Familial amyloid polyneuropathy III	Apolipoprotein AI (fragments)
Finnish hereditary systemic amyloidosis	Gelsolin (71 amino acid fragment)
Type II diabetes	Amylin (fragment)
Medullary carcinoma of the thyroid	Calcitonin (fragment)
Atrial amyloidosis	Atrial natriuretic factor
Hereditary non-neuropathic systemic amyloidosis	Lysozyme (whole or fragments)
Injection-localised amyloidosis	Insulin
Hereditary renal amyloidosis	Fibrinogen α-A chain, transthyretin, apolipoprotein AI, apolipoprotein AII, lysozyme, gelsolin, cystatin C
Amyotrophic lateral sclerosis	Superoxide dismutase 1 (wt or mutant)
Huntington's disease	Huntingtin
Spinal and bulbar muscular atrophy	Androgen receptor [whole or poly(Q) fragments]
Spinocerebellar ataxias	Ataxins [whole or poly(Q) fragments]
Spinocerebellar ataxia 17	TATA box-binding protein [whole or poly(Q) fragments]

1.1.1 Alzheimer's Disease (AD)

Dementia refers to a brain disease that causes steady decrease in memory, and social behavior abilities. The World Health Organization (WHO) states that Alzheimer's disease (AD) is the most common cause of dementia, contributing to 60-70% of cases. Due to the rapid incense in life expectancy and the inexistence of treatment, WHO predicts the number of people with dementia will reach 135.5 million by 2050 [9]. Ever since Alois Alzheimer described the disease as a long-term and gradual memory loss, autopsy results from AD patients indicate that amyloid plaques are one of the hallmarks of AD [10]. Later, it was revealed that polymerization of the amyloid beta protein (Aβ) plays a critical role in pathogenesis of AD [11]. Recent evidence from studies indicates Aβ plagues in fibril formation affect brain functions [12, 13]. Aβ, typically consists of 40 or 42 amino acids, is the product of cleavage by endoproteolysis of amyloid precursor protein (APP), a 695 residue protein found in both neuronal and normal cells [14]. Dr. Tian and his group defined how the APP and secretases act together to produce Aβ (Figure 1) [15]. Aβ Cascade hypothesis states that the APP mutation is one of the main causes of Aβ decomposition [16].

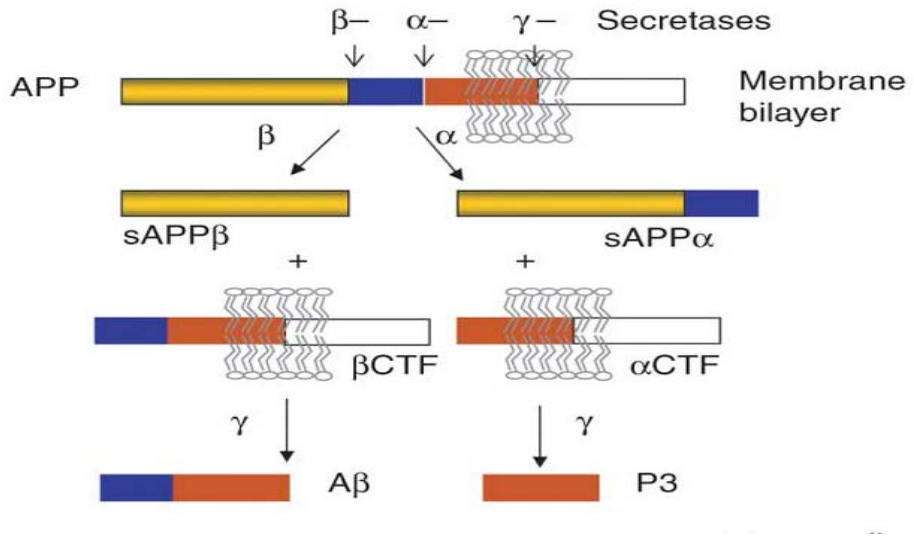

Figure1. The figure describes how Aβ is produced by endoproteolysis of APP. First, APP is cleaved by proteolytic enzymes: α, β, secretases. Then, γ secretase produces the C-terminal end of Aβ. This process determines the amino acid residues in length (30-51).

Although the exact normal function of Aβ is not well understood, the Aβ deposition by oligomers and fibrils will eventually lead to an accumulation of plaques in the brain [17 18]. In order to understand the deposition process of Aβ, it is important to recognize how Aβ assembles into fibril formation. Figure 2 represents both the aggregation phase of Aβ and the fibril development process [19]. From previous studies, it has been revealed that a fragment of the peptide (KLVFF) that residues on 16-20 of Aβ serves as a key recognition element for the formation of oligomers and fibrils [20]. With this known, numerous pharmacological approaches are being held to inhibit this region from interactions between Aβ proteins [21-23].

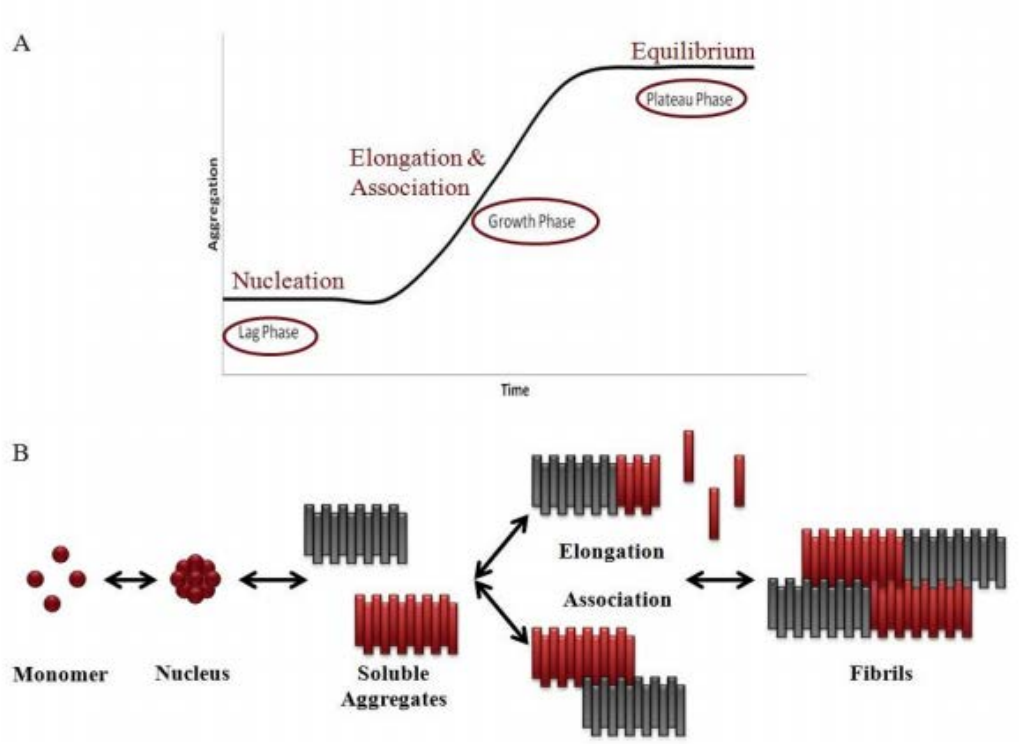

Figure2. Figure 2A is an aggregation graph of Aβ respect to time. Three phases are defined from the graph: lag phase, growth phase, and plateau phase. After growth phase begins, a rapid growth in Aβ aggregation is detected. Figure 2B shows how monomeric Aβ develops into fibril.

1.1.2 Type II Diabetes (T2D)

Type II diabetes (T2D) is a metabolic disease that is mainly found in adults after mid-age. T2D is associated with vascular diseases. About 90 % of diabetes cases are classified as T2D [24]. T2D is usually characterized by insulin disorder caused by the body cells and failure to absorb and use the Islet amyloid polypeptide (IAPP), secreted from pancreatic islet β-cells [25]. Due to the defects of β-cells, instead of being extracted via the kidneys, IAPP deposits in human cells [26]. Although biological actions of IAPP are not clearly understood, recent efforts discovered that IAPP is related to suppression of food intake, gastric emptying, and arginine-stimulated glucagon secretion [27-28]. As T2D proceeds, IAPP converts from a soluble monomer to β-sheet fibril like Aβ protein [29]. Later, it was suggested that the interaction between IAPP fibril deposits and β-cell is associated with β-cell death, which aggravates T2D symptoms [30]. Majority of T2D patients were treated with insulin therapy. Patients were injected with aggressive insulin to improve and preserve β-cell with reduced resistance [31]. Current researches take alternate approaches to inhibit the aggregation of IAPP and various inhibitors are proven to work in *vivo/ in vitro* [32-36]. Like Amyloid beta, IAPP aggregation is related with certain sequence of the protien: residue 20-29 [34].

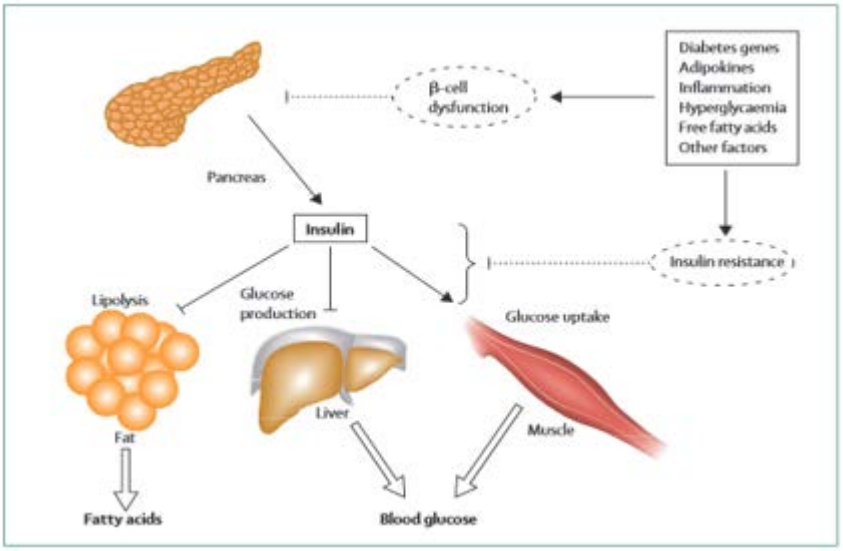

Figure3. Pathology of hyperglycaemia and increased circulating fatty acids in T2D.

1.2 What is a Peptoid?

Peptides have been closely related to drug discoveries and have been studied for decades, since Dr. Merrifield found a way to add amino acids to growing peptide chains [37]. Poly N-substituted glycine (peptoid) is a class of peptide mimetics that has a similar backbone structure with peptide, but side chains are attached to nitrogen instead of the α-carbon [38]. This structure gives peptoids flexible of backbone structures and reduced bio-degradability. With the inclusion of α-chiral and aromatic residues, helical structures can be incorporated into peptoids, thus stabilizing the structure [39, 40]. Unlike peptides, the second structures of peptoids are not stabilized by hydrogen bonds, which can be denatured. Peptoids, however, are stabilized by the steric hindrance that is less vulnerable *in vivo* [41]. This makes peptoid more resistant to the proteolytic activities. Also, due to inclusion of the side chains through SN2 displacement, a larger variety of side chain chemistries can be attached to peptoid than can be attached to peptides [42].

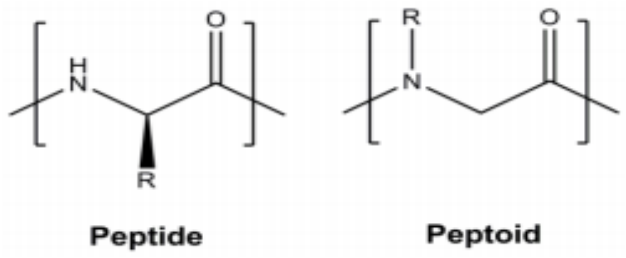

Figure3: Comparison between peptide and peptoid. Whie the side chain of peptid is attached to α-carbon, side chain of peptoid is attached to nitrogen giving more flexibility to the backbone structure.

Side chain chemistry and sequence determine the peptoid's water solubility, helical content, and side chain bulk [43]. As such, peptoids are used in biological fields including drug/drug delivery science, catalysts, and biomaterials [44-47]. Furthermore, pharmaceutical companies have been actively developing peptoid drugs after the success of Chiron in applying peptoids to their drug products [48-49]. Currently, peptoids are emerging as novel compounds for neuroscience with greater selectivity of drug actions with less side effects.

2. Previous research on misfolded proteins

As mentioned earlier, various efforts have been made to inhibit the aggregation of misfolded proteins. The secondary, tertiary structures of proteins serve as a hallmark for PCDs. Reducing these hallmarks are the main targets in developing novel therapeutic methods to cure the diseases. Since the exact cause of protein misfolding is unknown, it is hard to prevent the initiation of misfolded protein. Current research suggests novel compounds/methods to inhibit the aggregation of the proteins, which is believed to be the major pathological cause of PCDs.

2.1 Chaperone

i. Chaperone from *E. coli*

Chaperones refer to proteins that are related to the normal folding process in endoplasmic reticulum (ER) [50]. Different kinds of chaperones prevent misfolded proteins from exporting out of the ER system by recognizing their redundant structures [51-52]. When such step fails, misfolded proteins can be exported from ER and undergo aggregation rapidly [53]. While there are chaperones in human bodies, bacteria also contain chaperones. Most of these bacteria are called heat shock proteins (Hsp) [6]. Hsp90, Hsp70, and Hsp 60 are major chaperons in bacteria like *E. coli*., which are involved with the damage-controlling functions [54-56]. These Hsps were tested in *E.coli* and proven to break the insoluble aggregates in a short period [57]. With these researches, Hsp70, 90 are suggested as new pharmaceutical approaches for diseases caused from misfolded proteins.

ii. Chemical Chaperone

Denning and colleagues have discovered that temperature can affect mutation conformation by comparing maturity of cystic fibrosis transmembrane conductance regulator (CFTR) at four different temperatures. They have found out that CFTR at residue 538 is showing less maturity at high temperature synthesizing more misfolded proteins [58]. Inspired by Dennig's work, Brown and his colleagues conducted research

to prove that CFTR mutations can be inhibited by low molecular weight compounds that are known to stabilize proteins in native conformations [59]. With this theory, recent researchers found other chemical chaperones (Glycerol, *N*-octyl-h-valienamine, DMSO, and TMAO) that can inhibit the misfold proteins [60-64].

2.2 Gold nanoparticles

Gold is a well-known inert material that has resistance toward chemical reaction and oxidation. With this property and small size that enhance the biocompatibility, gold is widely used in bio application: bio-sensing, imaging technology, and optoelectronics [65-67]. After Turkevitch, et al. have succeeded in synthesizing gold nanoparticles (AuNPs) by reducing Au (III) to Au (0) in water using citrate, many scientists have developed various ways to synthesize the AuNPs and to use it therapeutic purpose [68]. For decades, several of ligands were tested to find out the best formation of AuNP against misfolded proteins and results showed high inhibition characteristics [69-71]. Liao, et al. found that high negative charge density inhibits the fibril formation of Aβ and induce fibril dissociation [72]. Along its ability to decompose Aβ proteins, AuNP also demonstrates the ability to inhibit the fibrillation of IAPP [73].

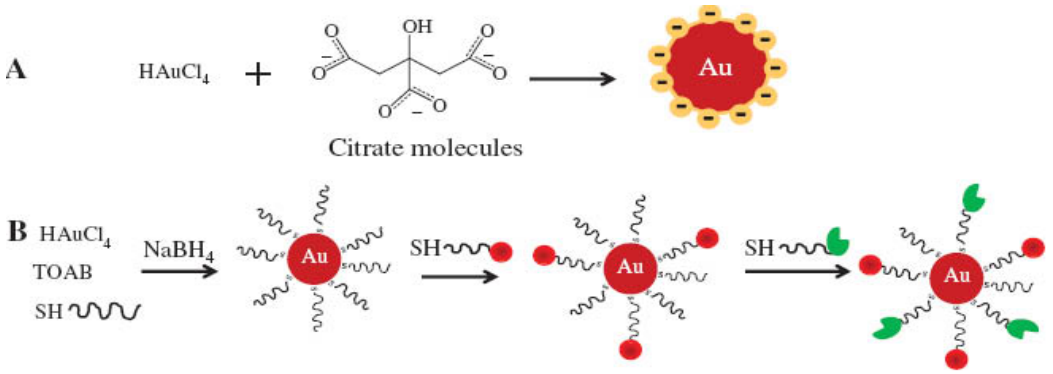

Figure 4: Figure 4.A is a synthesis for negative charged AuNP through reducing gold compound and, Figure 4.B is a synthesis to attach functional ligands upon the surface of AuNP.

2.2 Peptoids

Another novel approach to inhibit the aggregation of misfolded protein is to target the stacking sights of the misfolded proteins. Early approach suggested inhibiting the aromatic stacking of fibrils by injecting small aromatic molecules like Congo Red [74]. Later, the approach was developed to target only the binding sequences of proteins with peptides [75]. The peptoids were synthesized to target the binding sights of aggregates by mimicking the sequence that are closely related in bindings process. For example, the effective peptide inhibitors of Aβ mimic KLVFF sequence, a key fragment in fibril formation in secondary structure interaction [20, 76, 77]. As one of the promising peptide, I Aβ5 with a sequence of LPFFD has been designed and tested successfully *in vitro* [78]. However, due to its low bioavailability, it was limited to be used *in vivo* [79]. Dr. Servoss and her lab group studied the use of peptoids as Aβ inhibitor with the same principle. A peptoid with the sequence of KIIFFIFF (JPT1), where L and V amino groups are replaced with chiral I-like group and aromatic F groups to induce helical secondary structure, was proposed and tested under incubation with Aβ-40. As a result, the fibril inhibition of JPT1 was observed to inhibit Aβ-40 aggregation by decreasing the lag phase in Aβ nucleation. The Aβ-40 with JPT1 was characterized with reduced β-sheet formation, a key component in stacking process. The incomplete nucleation of Aβ also led to a shorter growth phase with a smaller aggregation amount [80]. Later, it was found that positively charged space of peptoid largely contributes to the inhibition of oligomerization while negatively charged spacer can alter oligomer structures [81].

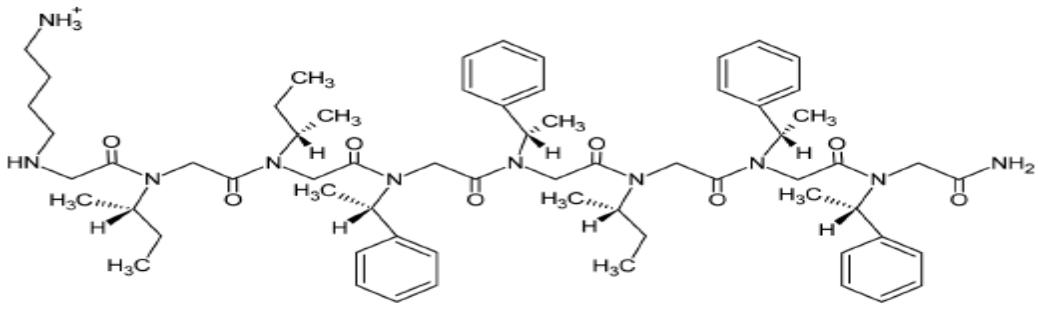

Figure 5: Structure of JPT1, with peptide sequence of KIFFFIFF

3. Modulating Amyloid-β Aggregation: The Effects of Peptoid Side Chain Placement and Chirality

3.1 Aim of Research

After Dr. Servoss' lab group has reported the use of peptoid (JPT1) in inhibiting Aβ aggregates, more investigations were required to understand the morphology of peptoids and increase its potential for therapeutic use [80]. In this research, JPT1 was modified to two different structures: JPT1s, JPT1a. JPT1s was designed to change the arrangement of aromatic (F-like) side chains. Instead of the previously studied sequence of JPT1 (KIIFFIFF), JPT1s was arranged with a sequence of IFFFIKIF. Since no side chain was added or removed, JPTs has the same molecular weight with JPT1. Instead, due to the aromatic side chains, it forms a different secondary structure with JPT1. While JPT1 has 6Å spacing between two adjacent aromatic groups, JPT1s has 12Å spacing between the aromatic structures located at opposite ends of a helix structure. JPT1a was designed so that it does not contain side chain chirality from JPT1. To make the compound achiral, methyl groups that were attached to α-carbon, were removed. Both Thioflavin T (ThT) and immunoblotting techniques will be used to observe changes to Aβ aggregation. ThT emits a high fluorescent signal in the presence of β-sheet structures, and immune blotting assay with OC can identify the presence of fibrillar conformations of misfolded proteins. [82].This research will provide a better understanding of the relationship between peptoid sequence/secondary structure and inhibition activity. The overall goal of this project is to find more information to build a more effective structure of peptoid as an Aβ inhibitor.

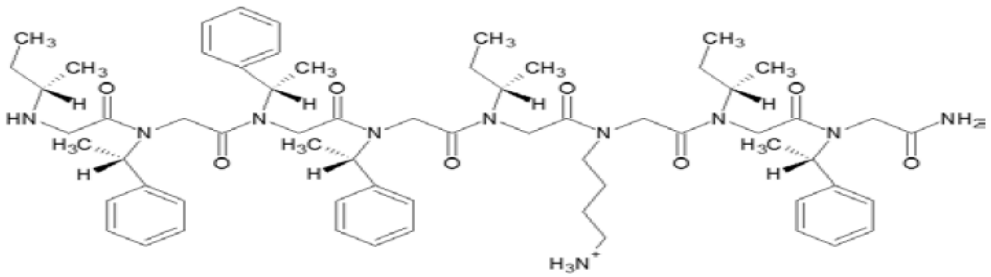

Figure 6: Structure of JPT1s, F-like side chains are rearranged from JPT1 (IFFFIKIF).

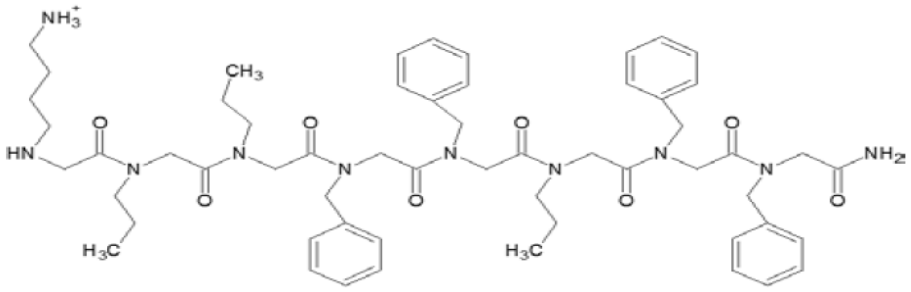

Figure 7: Structure of JPT1a, the achiral form of JPT1, methyl groups attached toα- carbon are removed.

3.2 Research methods

(* performed by J.P Turner, ** performed by Dongwon Park, *** performed by both)

*Peptoid synthesis& purification**

Peptoid JPT1, JPT1s, and JPT1a were synthesized by hand on rink amide resin. The resin will be swelled with dimethylformamide (DMF). The Fmoc protecting group was removed with 20% piperidine in N-methylpyrrolidinone. The peptoid backbone was attached by vortexing the resin in a mixture of 1.2 M bromoacetic acid in DMF and N, N'-diisopropylcarbodiimide in ratio of (5.3:1) for 60 minutes. The side chain amines were integrated by resin via an SN2 reaction mechanism. The side chain integration process was repeated until the desired peptoid sequence was obtained. When the synthesize was completed, the peptoid was removed from the resin using a mixture of 95% trifluoroacetic acid, 2.5% triisopropylsilane, and 2.5% water. The remainder acid on peptoid was treated by the rotating evaporator. The peptoids were purified using preparative high pressure liquid chromatography (HPLC). Gradients were run at ~1% per minute with 5−95% solvent B in A (A: water, 5% acetonitrile, 0.1% TFA; B: acetonitrile, 5% water, 0.1% TFA). Purity of each peptoids was confirmed by analytical HPLC with a gradient of 5-95% solvent D in C (C: water, 0.1 % TFA; D: acetonitrile, 0.1% TFA). Lastly, the mass of peptoid was measured by MALDI,-TOF mass spectrometry to be compared with theoretical mass. Finally, secondary structure of peptoids was confirmed by diluting the peptoids in methanol (120μM) and running circular dichroism at the scanning speed of 6 nm min^{-1} .

*Aβ Preparation****

Aβ-40 peptide was purchased and stored at -20 °C. The peptide was dissolved in 1, 1, 1, 3, 3, 3-Hexafluoro-2-propanol (1 mM) and set on ice for an hour. Then, the solution was divided into silicon coated vials and allowed to be evaporated overnight at room temperature. After the evaporation, each Aβ samplewas stored at -80 °C with desiccant. Prior to aggregation assay, each aliquot was treated with 18.7 μL of 5 mM sodium hydroxide, 347.7 μL of 40mM Tris hydrochloride buffer (Tris HCl; pH=8.0), and 13.6 μL of 4.4 M sodium chloride and incubated in ice for 10 min.

*Aggregation assay (ThT, Dot Blot, TEM)***

To make sample solutions, 20μL of each inhibitor (JPT1, JPT1s, and JPT1a) or dimethylsulfoxide (control) was added to each Aβ-40 aliquot. The sample solutions were placed on an orbital shaker at 800 rpm and room temperature. ThT and immunoblotting assays were performed simultaneously during the aggregation assay.

*Thioflavin T (ThT) assay***

For ThT assay, 0.0857 ml of 1 mM ThT stock solution was be mixed with 5.914 ml of Tris HCl to make a working solution. For each time point, 25 μL of collected from sample solutions and mixed with 175 μL of Tris HCl in a cuvette. The fluorospectrometer absorbance was performed at an excitation of 450 nm and emission of 490 nm.

*Dot blot****

For immunoblotting assay, antibody OC was used to detect Aβ fibrils. The samples for this assay were collected by dropping 2 μL of sample from each vial onto a nitrocellulose membrane sheet. After collecting the dot blot samples, the nitrocellulose membrane sheets were stored with 5% skim milk in Tris buffered saline with 0.2% of Tween20 (TBS-T) to protect the fibril form of samples. The samples were left in a 2 °C refrigerator for one day. Next, the Membranes were washed with TBS-T 3 times by using an orbit shaker. Antibody OC was diluted in the 5% skim milk (1:5000) and poured on the membranes. The membranes were then placed on an orbit shaker for an hour. The milk solution was washed with the TBS solution again 3 times. As a secondary antibody, alkaline phosphatase-conjugated anti-rabbit, diluted in

the 5% skim milk in ratio of 1:3000 was used to amplify the binding signal. The membranes were treated with the anti-rabbit for another hour on the orbit shaker. A mixture of 5-bromo-4-chloro-3-indolyl phosphate and nitrobluetetrazoliumchloride was used to develop the dots. After 5 minutes of incubation, 10 % acetic acid was used to stop further reaction. The dot intensity was measured by scanning the dots with a scanner and ImageJ, a program that calculates the intensity of color.

*Transmission electron microscopy (TEM)**

To collect TEM samples, 300 square mesh nickel grid was purchased. Samples (3µL) were spotted on a parafilm and the grid was placed on the top of sample with the nickel side facing the bottom for one minute. A piece of filtration paper was used to soak the excess stain on the surface of grid. With the same method, the grid was placed on the top of 2% uranyl acetate (3µL) for 45 seconds. The excess uranyl acetate stain was treated with filtration paper. TEM imaging was performed with JEOL-011 TEM at a voltage acceleration of 110kV.

3.3 Results and discussions

Molecular secondary structure observance by CD.

As previously discussed, JPT1 contains the secondary helix structure with ~12 Å distance between F-like side chains. This structure can be easily detected using CD. It is critical to check the helicity of JPT1s and JPT1 to observe the importance of helical spacing in acting against pi-pi stacking of Aβ.

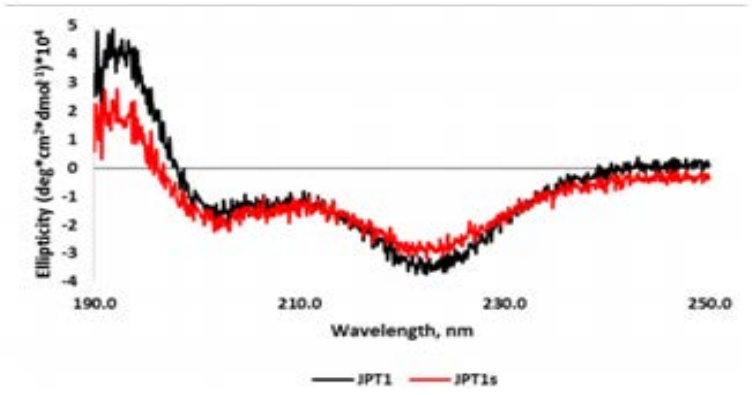

Figure 8: Curves in circular dichroism spectrum for JPT1 and JPT1spresenthelical secondary structures

Comparison of Peptoids inhibition capacity (JPT1, JPT1s, JPT1a)

The ThT aggregation was performed with a control (20 μM of Aβ) and Aβ sample, where100 μM of JPT1, JPT1s, or JPT1a is injected individually. Through the ThT Fluorescence emission, the quantity of misfolded proteins can be observed. The enhanced fluorescence represents the presence of fibilization of β-sheet structures. The following figure displays the fluorescence graph of each sample. From this data, it can be observed that the control does not begin its growth phase until the 60 min period. After 60 min, the control showed a sudden increase of β-sheet structure while the samples treated with peptoids did not show a noticeable increase in β-sheet structures. The Aβ samples where the peptoids were injected had significantly lower fluorescence signal than the fluorescence of the control (Aβ). Another intriguing pattern shown on the fluorescence graph was the relationship between the lag phase and fluorescence at plateau. Comparing the peptoid inhibiting performances, it is shown that JPTs and JPT1a show a similar pattern to that of JPT1. However, the JPT1s show a longer lag phase with less inhibition rate compared to those of other two peptoids.

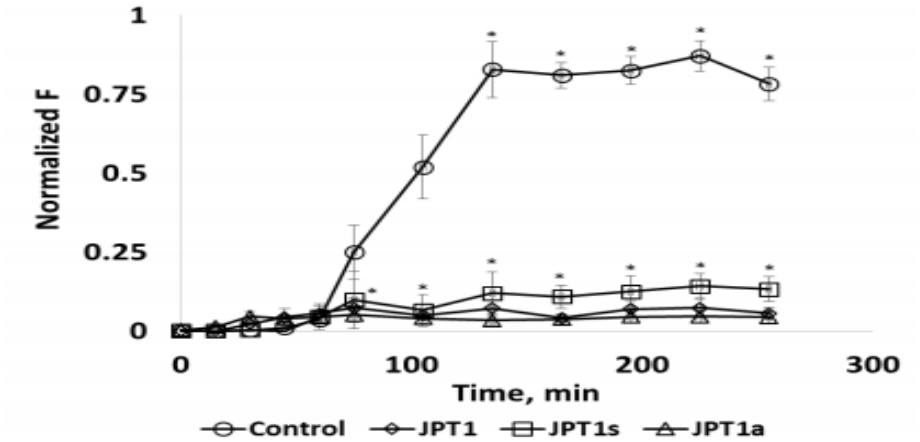

	JPT1	JPT1s	JPT1a
% Inhibition	83.1 ± 4.8^{+++}	76.9 ± 4.8^{+++}	85.6 ± 4.8^{+++}

Figure 9: ThT assay indicates that JPT1and its variants inhibit the β-sheet structures significantly through normalize ThT fluorescence. Each line represents the β-sheet structures of Aβ-40 (20 μM) with 100 μM of JPT1The aggregation assay was performed on an orbit shaker with 800 rpm.* indicates data points used for calculation of percent inhibition.

Likewise, the dot blot assay confirmed that peptoids inhibit the fibril formation of Aβ-40 with antibody OC .The secondary antibody, alkaline phosphatase-conjugated anti-rabbit, is a useful tool in analyzing proteins in that it can amplify the signal and the make the fibril forms detectable. In terms of dot density, the samples with peptoid showed less of dot densities than the control. From the data, JPT1 showed 46% of inhibition compared to that of control, while JPT1a, peptoid with lack of chirality, exhibited 72.6 % of inhibition rate. This result correlates with the ThT assay, where JPT1a exhibited a higher inhibition rate (85.6%) than JPT1 (83.1%). The inhibition pattern agrees with the ThT assay, where reduced lag phase contributes to the immaturity of fibrils.

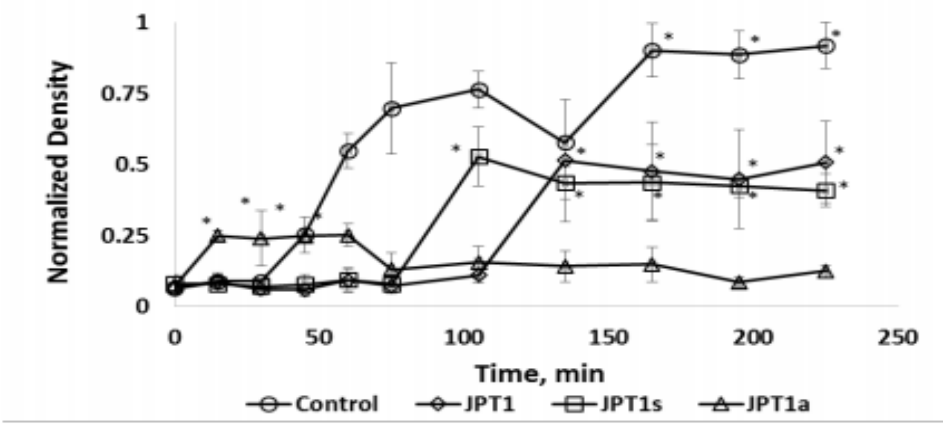

	JPT1	JPT1s	JPT1a
% Inhibition	$46.0 \pm 11.4^{\dagger\dagger}$	$50.5 \pm 9.0^{\dagger\dagger}$	$72.6 \pm 4.5^{\dagger\dagger,\phi}$
Fold-Change	2.7 ± 0.8	2.2 ± 0.3	<0.5

Figure 10: The fibril formation of Aβ-40 is quantified by Immunoblotting assay with antibody OC. JPT1a exhibits the highest inhibition rate. Normalized dot density is calculated as a fraction of the control plateau.. * indicates data points used for calculation of percent inhibition.

Lastly, TEM images were used to observe the reduction of fibril formation that are quantified by dot blot analysis. The samples for TEM imaging were collected when the fluorescence samples reached to the plateau stage since the dot densities could not be quantified during the aggregation performance. The decrease of fibril forms were observed with the addition of peptoids. The TEM image of the control (Figure 11.A) displays branches that are considered to be fibrils. The fibrils are reduced as the peptoids

were added (Figure 11. B-D). While the TEM image proved that the peptoids can inhibit the fibrilization of Aβ-40, it also showed that the Aβ-40 aggregates form different morphologies with JPT1a. The additions of JPT1 and JPT1s (Figure11 A, B) both result in small aggregates with significantly less number of branches. However, the aggregates formed with the JPTa (Figure11 D) contain some distinct characteristics that compared to the other two aggregates. While JPTa reduced the outer branches, it formed compact circular shape aggregates. A large aggregate at the bottom left corner of TEM image (Figure14 D) forms a bird nest-like morphology.

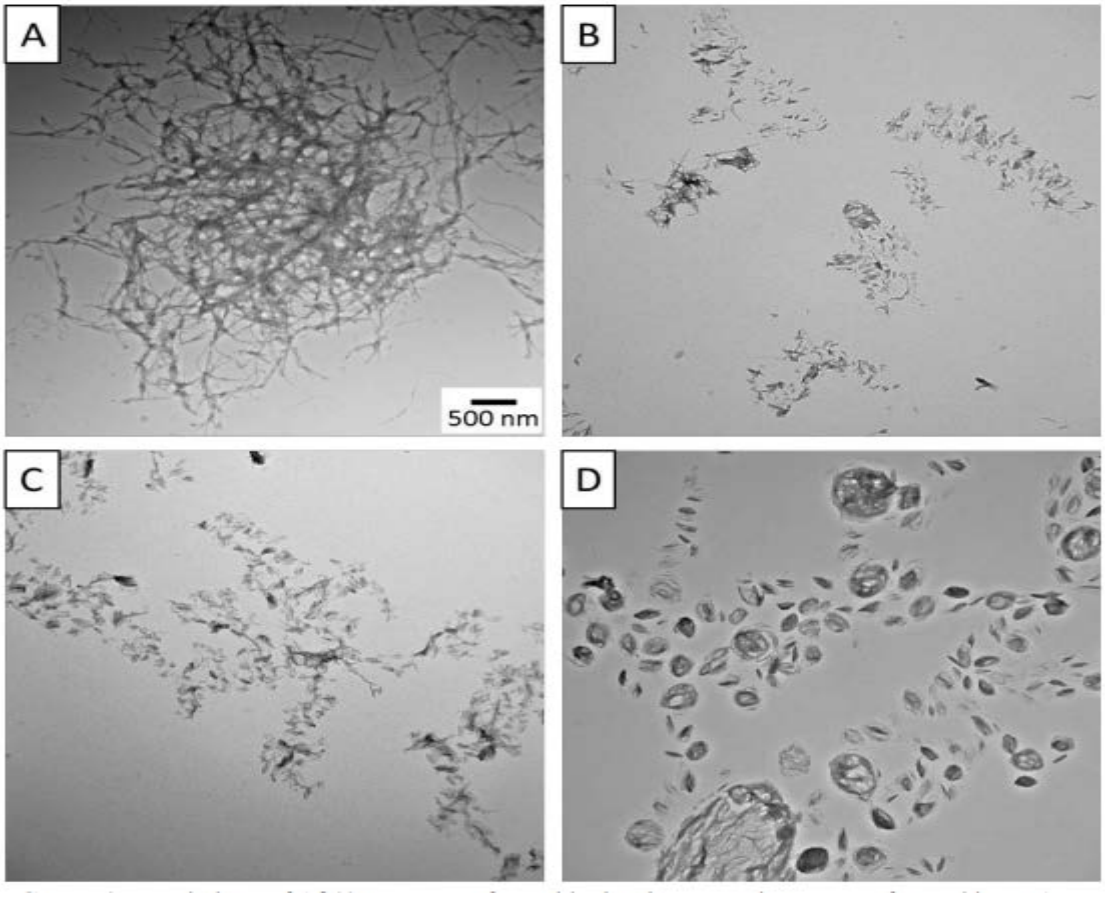

Figure 11: The morphology of Aβ-40 aggregates formed in the absence and presence of peptoids JPT1 (A), JPT1s (b), and JPT1a. (c). in 40 mMTris-HCl (pH 8.0) after plateau phases are reached.Results are representative of 3 independent experiments and imaged grid locations were randomly selected. Scale bars are 500 nm

3.4 Conclusions & Discussion

The experiment shows the inhibition capacity of variants of JPT1 (KIFFIFF) in different morphologies. While the research displays similar results that have been observed by previous works, it also shows how chirality and side chain replacement can affect the fibril inhibiting performance of peptoids [80]. The ThT assay, Dot blot assay, and TEM imaging conclude that the both variants of JPT1 act as Aβ-40 inhibitors. From experimental data, the rearranging the side chains (JPT1s) shows minimal effect on the JPT1's inhibiting capacity. However, it decreases the lag phase time in dot blot assays, exhibiting 4.5 % more inhibition capacity in the fibril development. As another variant, removing chirality of JPT1structure (JPT1a) notably affects the inhibiting capacity of JPT1. This change in the secondary structure prevents the helical structure of JPT1. JPT1a is characterized with a higher rate in inhibiting both β-sheet structures and fibril formation of Aβ-40 than that of JPT1. However, the TEM image of JPT1a develops a unique morphology of aggregates. It is suggested that trans conformation of JPT1a with an increase in its backbone flexibility is related to the increase of inhibition rate. The distinctive aggregate form of Aβ-40 with a presence of JPT1a can be explained with the research of Dr.Wu, et al. He observed that in certain cases, Aβ can change into high order oligomers than fibrils [83]. In this research, it is suggested that the achiral structure of JPT1 can reduce fibrilization of Aβ-40 forming a highly ordered aggregates.

4. Amyloid Beta Peptoid Inhibitor Prevents fibril Formation of Islet Amyloid Polypeptide

4.1 Aim of Research

Like Alzheimer's disease, T2D is a type of PCD, where the aggregation of islet amyloid polypeptide (IAPP), known as amylin, is observed as a hallmark of pathology. Aggregated IAPP fibril plays a critical role in delaying gastric emptying and inhibiting glucagon secretion. In previous studies, JPT1, a peptoid designed to mimic the binding sequence of Aβ, was observed to inhibit Aβ aggregation. While Amylin has a different sequence and a binding site than Aβ, the fibrilization mechanism of Amyllin is similar to that of Aβ. Both mechanisms develop from monomers to fibrils via β-sheet structure. With this theory, disrupting pi-pi stacking of IAPP is suggested to reduce fibril formation of amylin [84]. From this view, the same JPT1 used in inhibiting Aβ aggregation was to be tested for IAPP aggregation. This study was conducted to investigate the performance of Aβ inhibitor (JPT1) in IAPP *in vitro*. Since the formation of β-sheet structure is closely related to the fibril formation, ThT assay was performed along with TEM imaging. This study of inhibitor will help in understanding the inhibitor's mechanism and suggest wide application of a possible therapeutic compound (JPT1). Both free acid and aminated form of amylin were tested, since human IAPPs randomly consist of both forms. Also, a competition assay was performed to determine whether the JPT1 was competitive with ThT binding by fibrils.

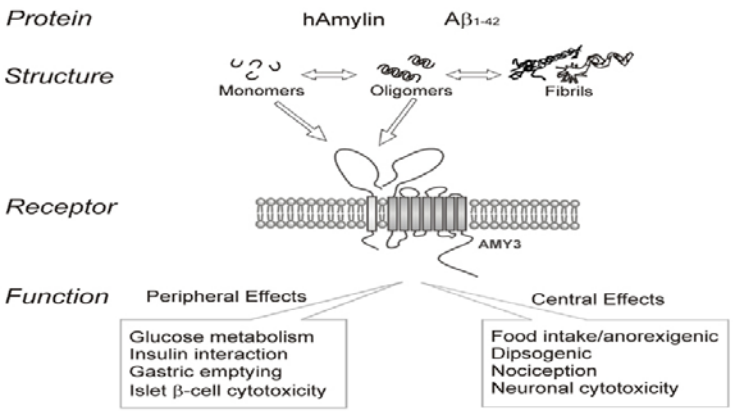

Figure 12. The image describes the similarity between human IAPP and amyloid beta protein.

4.2 Research methods

Peptoid synthesis& purification

The same JPT1 from the previous research has been used for this experiment.

*Amylin Preparation****

Both free acid and aminated amylin were purchased and stored at -20 °C. The amylin was dissolved in 1, 1, 1, 3, 3, 3-Hexafluoro-2-propanol (1 mM) and set on ice for an hour. Then, the solution was divided into silicon coated vials (0.0286 mg) and allowed to evaporate overnight at room temperature. After the evaporation, each Amylin sample was stored at -80 °C with desiccant. Prior to aggregation assay, each aliquot was treated with 0.15 µL of 5mM sodium chloride and 366.15 µL of 40 mM sodium phosphate (pH 8), resulting in a 20 µM total amylin concentration. Each amylin aliquot was incubated in ice for 3 hours.

*Aggregation assay (ThT, TEM)****

Before agitation, different amounts of JPT1 were added to each amylin aliquot (0 µM. 40 µM, 70 µM, 100 µM) and dissolved for 10 min. The samples were placed on an orbital shaker at 400 rpm and room temperature. ThT assay was conducted while the TEM imaging sample was collected.

Competition assay

To perform the competition assay, a standard fibril sample was prepared by agitating both free acid and aminated version amylin control on the orbit shaker at 400 rpm. To ensure the complete fibrilization of each amylin type, free acid amylin was set on the shaker for 3 days and aminated amylin was set for 5 days. The fibrils were separated by a centrifuge machine at 14.5 krpm for 15 mintues. The supernatant was carefully separated from the solution by removing solutions. The fibrils were diluted to 50 µM with the same buffer solution used in sample preparation and sonicated for 30 seconds. For ThT sample solution, 2.5 M of fibril was mixed with 37.5 M of ThT with different concentrations of JPT1. Samples were measured at 5 minutes, and 180 minutes after mixing to check if the JPT1 does not affect the ThT binding site over time. The fluorospectrometer absorbance was performed at an excitation of 450 nm and emission of 490 nm.

*Thioflavin T (ThT) assay****

For ThT assay, 0.07 ml of 1 mM ThT stock solution was be mixed with 4.93 ml of Tris HCl to make a 5 ml of working solution. For each time point, 25 μL of collected from sample solutions and mixed with 175 μL of working solution in a cuvette. The fluorospectrometer absorbance was performed at an excitation of 450 nm and emission of 490 nm

*Transmission electron microscopy (TEM)**

Carbon coated 400 square mesh nickel grids were purchased for TEM imaging. Before using the grids as sample plates, they were treated with acetone nitrile for one hour. For a sampling, 3μL of solution from each vial was directly spotted on a nickel grid for one minute. A piece of filtration paper was used to soak the excess stain on the grid surface. After removing the stain, 1% uranyl acetate (2μL) was placed above the grid for 45 seconds. The excess uranyl acetate stain was treated with filtration paper. TEM imaging was performed using a JEOL-011 TEM with a CCD camera at voltage acceleration of 110kV.

4.3 Results and discussions

Competition assay

The competition assay was performed to observe whether JPT1 is competitive with ThT and fibril interaction. A complete fibril formation of each amylin was produced by agitating aggregation samples for 3 days (aminated version) and 5 days (free acid version) on the orbit shaker (400rpm). ThT fluoresce of each sample was measured after adding different concentrations of JPT1. The samples were measured at different times (5 min, 180 min). In order to observe whether the JPT1 is competitive with ThT for certain period of time, the fluoresces of the samples were measured at different times. The following data for aminated type amylin indicates that JPT1 is competitive with ThT and amylin binding. It was observed that the fluoresces of both types of amylin are not dependent on the concentration of JPT1. In addition, the increase of JPT1 concentration also did not affect the fluoresce neither. This concludes that JPT1 does not affect the binding site of ThT and the β-sheet structure. Although a noticeable drop of fluoresce was observed after 180 min of incubation, fluoresce was not dependent on JPT1 concentration.

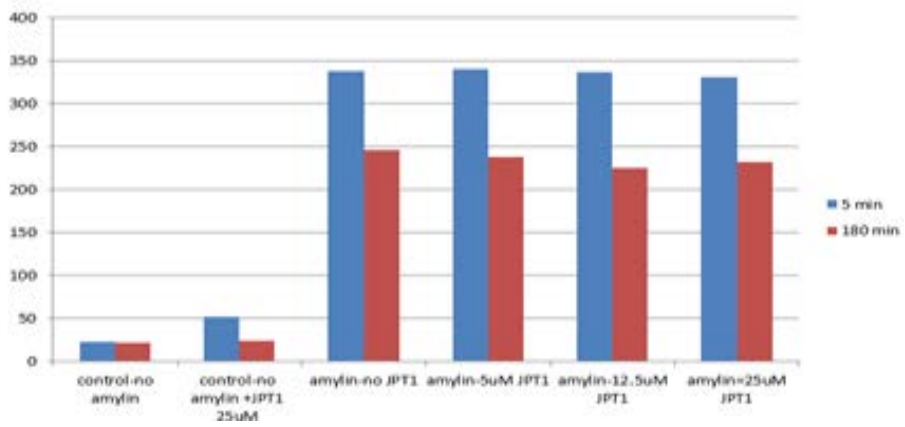

Figure 13. This is competition assay of 50 μM of aminated amylin that has been set on orbit shaker for 2days. ThT essay was used to observe whether Thioflavin T binds with JPT1 in final concentraiton of 37.5μM. THe fluorescence for each vial was measured after 5, 180 min after JPT1 was added. The graph presents that ThT fluorescence is not affected by the concentration of JPT1.

Competition assay for free acid amylin was performed in the same manner. Experimental data indicates JPT1 does not affect the ThT binding, showing the same pattern with that of aminated amylin. However, unlike aminated amylin, free acid amylin is not characterized with a drop between 5 min (blue) and 180 min (red). This concludes that β-sheet structure of free acid amylin is more stable in ThT environment than that of aminated amylin. From this data, it is also concluded that free acid amylin forms less β-sheet structure than aminated amylin when complete fibril forms are developed.

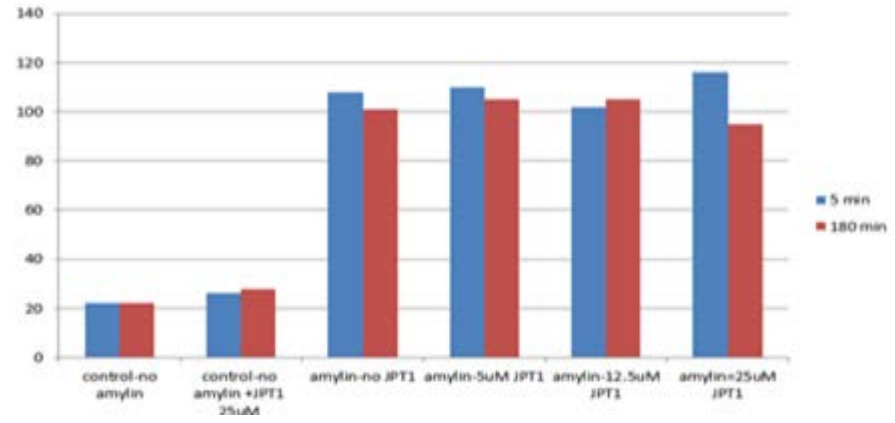

Figure 14. This is competition assay of 50 μM of free acid amylin that has been set on orbit shaker for 2days. ThT essay was used to observe whether Thioflavin T binds with JPT1 in final concentration of 37.5μM. THe fluorescence for each vial was measured after 5, 180 min after JPT1 was added. The graph presents that ThT fluorescence is not affected by the concentration of JPT1.

JPT1 performance in inhibiting beta-sheet structures and fibrils of amylin (aminated, free acid)

ThT assay

It has been proved that the JPT1 does not interrupt the binding site of ThT with beta sheet structure of both types of amylin through competition assay. Because of this, ThT assay was performed to check the inhibiting capacity of JPT1 against the amylin aggregation. ThT assay was performed by comparing ThT fluoresce of a control (20 μM of Amylin) with samples treated with different amount of JPT1 (40 μM, 100 μM, 200 μM). From previous research by Dr. Lutz-Rechtin, the ThT fluorescence plateaus of aminated amylin were observed around 10 hours of agitation (400 rpm) while the plateaus were observed around 20 hours of agitation (400 rpm) for free acid version. Figure 15 presents the ThT fluoresce graph of aminated amylin samples for 10 hours. While JPT1 treated Aβ samples were characterized with their shortened lag time (Figure 9), ThT assay for amylin did not display noticeable differences in the lag times with respect to JPT1 concentrations. However, a clear decrease of fluoresce was observed as more JPT1 was added into aminated amylin.

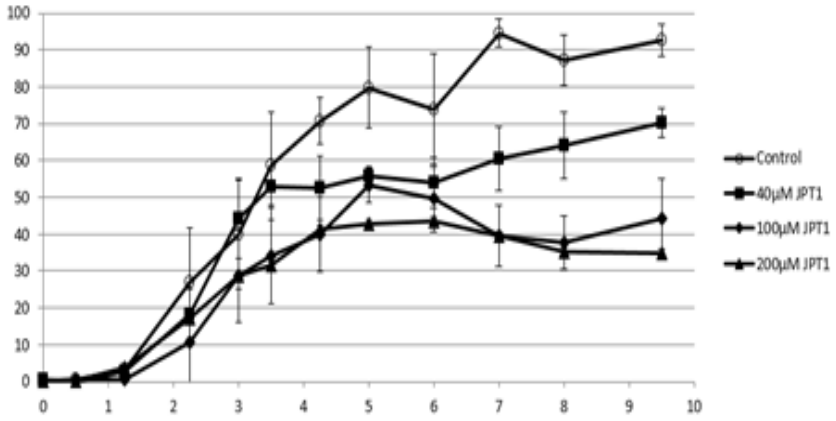

Figure 15. ThT Fluorescence graph quantifies beta sheet formation of amylin. JPT1 was added to the 20 μM aminated amylin in concentration of 0, 40, 100, 200 μM. The data represent mean of four independent ThT assays

Although ThT fluoresce graph of aminated amylin confirmed a distinct relationship between β-sheet formation and JPT1, the following fluoresce graph of free acid amylin did not abide with the aminated

amylin. A decrease in beta sheet structure was observed only to 100 μM concentration of JPT1. Unlike its behavior in aminated amylin, JPT1 presented almost no inhibition capacity in a concentration of 200μM.

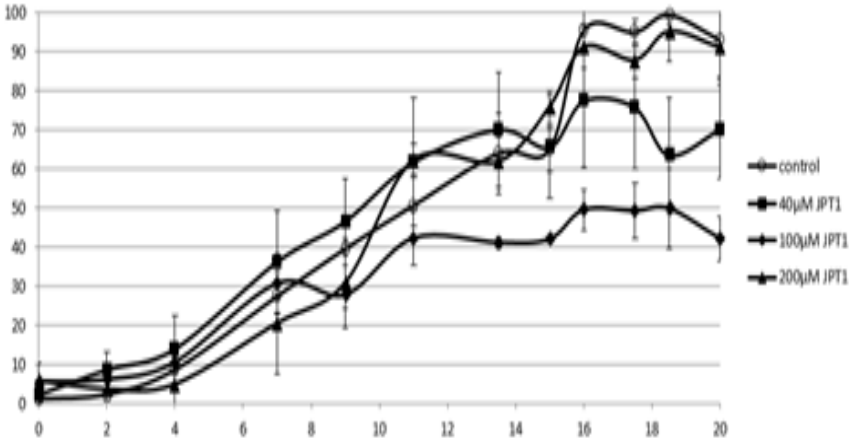

Figure 16. ThT Fluorescence graph quantifies beta sheet formation of amylin. JPT1 was added to the 20 μM free acid amylin in concentration of 0, 40, 100, 200 μM. The data represent mean of four independent ThT assays.

TEM

The following TEM images are from free acid amylin samples collected at three different times. Each row represents different concentration of JPT1 in 20μM of Amylin. Within each row, the first picture is a sample collected at the end of growth phase; the second picture is a sample collected when the plateau stage was observed; the third picture is a sample collected after 5 days of incubation. A clear decrease in fibril branches was observed with free acid amylin with 40 μM of JPT1. Similarly, free acid amylin with 100 μM of JPT1 inhibited fibrils formation of free acid amylin at plateau stage. However, as those oligomers develop, high order oligomer form was observed after 5 days of incubation. This pattern was also observed in free acid amylin with 200 μM of JPT1; no fibril was detected at the plateau stage and agglomerates with different morphology were detected after 5 days of incubation.

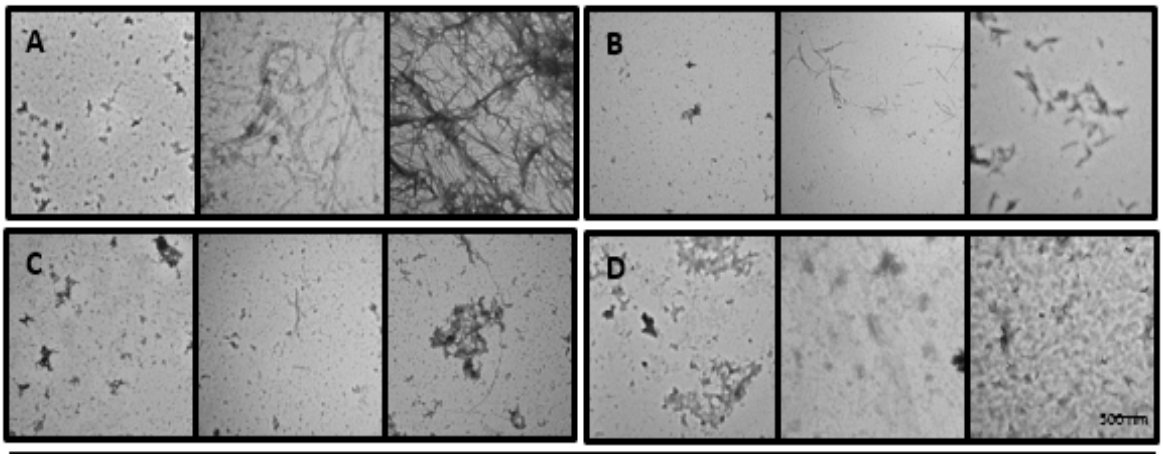

Figure 17. The morphology of free acid amylin aggregates formed in the absence and presence of peptoids JPT1 (A), 40 μM of JPT1 (B). 100 μM of JPT1 (C) 200 μM of JPT1 (D) in 40 mMTris-HCl (pH 8.0). The first picture in each row is image of sample that was collected when growth phase was ended and the second picture is image of sample collected at plateau. The last picture of each row was from samples collected 5 days after aggregation. Imaged grid locations were randomly selected. Scale bars are 500 nm

4.4 Conclusion/Discussion

In this research, JPT1 was performed against amylin misfolded aggregation, a hallmark of T2D. The performance of JPT1 was already tested in Aβ aggregation environment and it was concluded that JPT1 inhibits β-sheet structure and fibril forms of Aβ [80]. Although JPT1 was designed after the binding sight of Aβ, its secondary structure that interrupts pi-pi stacking of misfolded protein seemed to be applicable in inhibiting aggregation of amylin. To test this theory, ThT assay and TEM imaging were performed for both aminated and free acid amylin. Competition assay was conducted before ThT assay to validate that JPT1 does not affect binding between ThT and β-sheet for both types of amylin. The result showed that fluorescence signals are not affected by concentration of JPT1 for both amylin. Through the ThT assay, it was proven that JPT1 inhibits the aminated amylin β-sheet structure with respect to its concentration. However, only a certain range of JPT1 concentration (40, 100μM) contributed to inhibit β- sheet formation of free acid amylin. From the TEM images, free acid amylin samples with a high concentration of JPT1 were observed to have a decreased number of fibrils. However, the aggregates had distinct morphologies. This characteristic concedes to the oligomer growth phase that was mentioned by Dr.

Green, et al. From her research, Dr. Green observed protofibrils when the growth of amylin was constrained [85]. While there is not a clear answer for the toxicity of high order oligomers, the morphologies of high order oligomers are believed to cause disruptions in human body metabolisms due to agglomerates with high density. Overall, this study concludes that fibril formation of both amylin types can be inhibited by amylin. However, dosage studies are required to prevent the high order oligomer form.

A.1 REFERENCE

1. Nelson DL, Cox MM (2005). *Lehninger's Principles of Biochemistry* (4th ed.). New York, New York: W. H. Freeman and Company
2. Dobson, C. M. (2003). Protein folding and misfolding. *Nature*, *426*(6968), 884-890.
3. Barral, J. M., Broadley, S. A., Schaffar, G., &Hartl, F. U. (2004). Roles of molecular chaperones in protein misfolding diseases. In *Seminars in cell & developmental biology* (Vol. 15, No. 1, pp. 17-29). Academic Press.
4. Chiti, F., & Dobson, C. M. (2006). Protein misfolding, functional amyloid, and human disease. *Annu. Rev. Biochem.*, *75*, 333-366.
5. NeuroPhage. (n.d.). Protein Misfolding Diseases - NeuroPhage. Retrieved April 15, 2016, from http://neurophage.com/science/protein-misfolding-diseases/ Chaudhuri, T. K., & Paul, S. (2006). Protein-misfolding diseases and chaperone-based therapeutic
6. approaches. *FEBS Journal*, *273*(7), 1331-1349.
7. Ross, C. A., & Poirier, M. A. (2004). Protein aggregation and neurodegenerative disease. *Nature Medicine* 10, S10–S17
8. Soto, C. (2001). Protein misfolding and disease; protein refolding and therapy. *FEBS letters*, *498*(2), 204-207.
9. World Health Organization (2015) Dementia Fact sheet N 362.
10. Dahm, R. (2006) Alzheimer discovery. *Curr Biology. 16*: 906-910
11. Selkoe, D.J (1994) Alzheimer's Disease: A Central Role for Amyloid. *Journal of .Neuropathol and Exp.Neurol. 53*: 438-447
12. Glenner, G. G., & Wong, C. W. (1988). Alzheimer's disease: initial report of the purification and characterization of a novel cerebrovascular amyloid protein. *Alzheimer Disease & Associated Disorders*, *2*(2), 134.
13. Masters, C. L., Simms, G., Weinman, N. A., Multhaup, G., McDonald, B. L., &Beyreuther, K. (1985). Amyloid plaque core protein in Alzheimer disease and Down syndrome. *Proceedings of the National Academy of Sciences*, *82*(12), 4245-4249.
14. Hardy, J.; Selkoe, D.J. (2002) The Amyloid Hypothesis of Alzheimer's Disease. Progress and Problems. *Science.* 297: 353-356
15. Tian, Y., Bassit, B., Chau, D., & Li, Y. M. (2010). An APP inhibitory domain containing the Flemish mutation residue modulates [gamma]-secretase activity for A [beta] production. *Nature structural & molecular biology*, *17*(2), 151-158.
16. Murrell, J., Farlow, M., Ghetti, B., & Benson, M. D. (1991). A mutation in the amyloid precursor protein associated with hereditary Alzheimer's disease.*Science*, *254*(5028), 97-99.
17. Hiltunen M, van Groen T, Jolkkonen J (2009). "Functional roles of amyloid-beta protein precursor and amyloid-beta peptides: evidence from experimental studies". *Journal of Alzheimer's Disease* 18 (2): 401–12.
18. Tjernberg, L. O.; Naslund, J.; Lindqvist, F.; Johansson, J.; Karlstrom, A. R. (1996) Arrest of Amyloid β Fibril Formation by a Pentapeptide Ligand. *J. Biol. Chem. 271*: 8545-8548
19. Moore, K. A. (2013). Gold Nanoparticles and Peptoids as Novel Inhibitors of Amyloid Beta Aggregation in Alzheimer's Disease.
20. Funke, A.; Wilbord, A.; Wilbord, D. (2012) Peptides for Therapy and Diagnosis of Alzheimer's

21. Näslund, J., Schierhorn, A., Hellman, U., Lannfelt, L., Roses, A. D., Tjernberg, L. O. ...&Greengard, P. (1994). Relative abundance of Alzheimer A beta amyloid peptide variants in Alzheimer disease and normal aging. *Proceedings of the National Academy of Sciences*, *91*(18), 8378-8382.
22. Stains, C. I., Mondal, K., & Ghosh, I. (2007). Molecules that Target beta-Amyloid. *ChemMedChem*, *2*(12), 1674-1692.
23. Yamin, G., Ono, K., Inayathullah, M., &Teplow, D. B. (2008). Amyloid β-protein assembly as a therapeutic target of Alzheimer's disease. *Current pharmaceutical design*, *14*(30), 3231-3246.
24. National Collaborating Centre for Chronic Conditions UK. (2008). Type 2 diabetes.
25. Vijan, S. (2010). Type 2 diabetes. *Annals of internal medicine*, *152*(5), ITC3-1.
26. Kahn, S. E. (2003). The relative contributions of insulin resistance and beta-cell dysfunction to the pathophysiology of type 2 diabetes. *Diabetologia*, *46*(1), 3-19.
27. Marzban, L., Park, K., &Verchere, C. B. (2003). Islet amyloid polypeptide and type 2 diabetes. *Experimental gerontology*, *38*(4), 347-351.
28. Jaikaran, E. T., & Clark, A. (2001). Islet amyloid and type 2 diabetes: from molecular misfolding to islet pathophysiology. *BiochimicaetBiophysicaActa (BBA)-Molecular Basis of Disease*, *1537*(3), 179-203.
29. Johnson, J. D., &Luciani, D. S. (2010). Mechanisms of pancreatic β-cell apoptosis in diabetes and its therapies. In *The Islets of Langerhans* (pp. 447-462). Springer Netherlands.
30. Meneghini, L. F. (2009). Early Insulin Treatment in Type 2 Diabetes What are the pros?.*Diabetes Care*, *32*(suppl 2), S266-S269.
31. Lorenzo, A., &Yankner, B. A. (1994). Beta-amyloid neurotoxicity requires fibril formation and is inhibited by congo red. *Proceedings of the National Academy of Sciences*, *91*(25), 12243-12247.
32. Thomas, T., Nadackal, G. T., & Thomas, K. (2003). Aspirin and diabetes: inhibition of amylin aggregation by nonsteroidal anti-inflammatory drugs. *Experimental and clinical endocrinology & diabetes: official journal, German Society of Endocrinology [and] German Diabetes Association*, *111*(1), 8-11.
33. Ward, B., Walker, K., &Exley, C. (2008). Copper (II) inhibits the formation of amylin amyloid in vitro. *Journal of inorganic biochemistry*, *102*(2), 371-375.
34. Mason, J. M., Kokkoni, N., Stott, K., &Doig, A. J. (2003). Design strategies for anti-amyloid agents. *Current opinion in structural biology*, *13*(4), 526-532.
35. Bennett, R. G., Hamel, F. G., & Duckworth, W. C. (2003). An insulin-degrading enzyme inhibitor decreases amylin degradation, increases amylin-induced cytotoxicity, and increases amyloid formation in insulinoma cell cultures. *Diabetes*, *52*(9), 2315-2320.
36. Merrifield, R. B. (1963). Solid phase peptide synthesis. I. The synthesis of a tetrapeptide. *Journal of the American Chemical Society*, *85*(14), 2149-2154.
37. Zuckermann, R. N., Kerr, J. M., Kent, S. B., & Moos, W. H. (1992). Efficient method for the preparation of peptoids [oligo (N-substituted glycines)] by submonomer solid-phase synthesis. *Journal of the American Chemical Society*, *114*(26), 10646-10647.
38. Kirshenbaum, K.; Barron, A. E.; Goldsmith, R.A.; et al (1998) Sequence-specific polypeptoids: A diverse family of heteropolymers with stable secondary structure. Proc. Natl. Acad. Sci. USA. 95: 4303-4308

39. Woo, C. W.; Sanborn, T. J.; Huang, K.; Zuckermann, R. N.; and Barron, E.A. (2001) Peptoid Oligomers with R-Chiral, Aromatic Side Chains: Sequence Requirements for the Formation of Stable Peptoid Helices. J. Am. Chem. Soc. 123: 6778–6784
40. Fowler, S.A.; Blackwell, H.E. (2009) Structure–function relationships in peptoids: Recent advancestoward deciphering the structural requirements for biological function. Org. Biomol. Chem. 7: 1508-1524
41. Turner, J. P., Lutz-Rechtin, T., Moore, K. A., Rogers, L., Bhave, O., Moss, M. A., &Servoss, S. L. (2014). Rationally designed peptoids modulate aggregation of amyloid-beta 40. *ACS chemical neuroscience*, *5*(7), 552-558.
42. Herbert, M.L.; Shah, D.S.; Blake, P.; Turner, J.P. (2013) Tunable peptoid microspheres: effects ofside chain chemistry and sequence. Org. Biomol. Chem. 11: 4459-4464
43. Lunt, B., Olivier, G., Pavinatto, F., Zuckermann, R., & Arias, A. C. (2013). Investigation of Peptoid Thin Films and Their Potential Use in a Biosensor.
44. Secker, C., Brosnan, S. M., Luxenhofer, R., &Schlaad, H. (2015). Poly (α-Peptoid) s Revisited: Synthesis, Properties, and Use as Biomaterial.*Macromolecular bioscience*, *15*(7), 881-891.
45. Lau, K. H. A. (2014). Peptoids for biomaterials science. *Biomaterials Science*, *2*(5), 627-633.
46. Lohan, S., & Singh Bisht, G. (2013). Recent approaches in design of peptidomimetics for antimicrobial drug discovery research. *Mini reviews in medicinal chemistry*, *13*(7), 1073-1088.
47. Zuckermann, R. N., Martin, E. J., Spellmeyer, D. C., Stauber, G. B., Shoemaker, K. R., Kerr, J. M., ... &Siani, M. A. (1994). Discovery of nanomolar ligands for 7-transmembrane G-protein-coupled receptors from a diverse N-(substituted) glycine peptoid library. *Journal of medicinal chemistry*, *37*(17), 2678-2685.
48. Ross, T. M., Zuckermann, R. N., Reinhard, C., & Frey, W. H. (2008). Intranasal administration delivers peptoids to the rat central nervous system.*Neuroscience letters*, *439*(1), 30-33.
49. Hughes, J., & Woodruff, G. N. (1992). Neuropeptides. Function and clinical applications. *Arzneimittel-Forschung*, *42*(2A), 250-255.
50. Barral, J. M., Broadley, S. A., Schaffar, G., &Hartl, F. U. (2004, February). Roles of molecular chaperones in protein misfolding diseases. In *Seminars in cell & developmental biology* (Vol. 15, No. 1, pp. 17-29). Academic Press.
51. McClellan, A. J., &Frydman, J. (2001). Molecular chaperones and the art of recognizing a lost cause. *Nature cell biology*, *3*(2), E51-E53.
52. Welch, W. J. (2004, February). Role of quality control pathways in human diseases involving protein misfolding. In *Seminars in cell & developmental biology* (Vol. 15, No. 1, pp. 31-38). Academic Press.
53. Hendrick, J. P., &Hartl, F. U. (1993). Molecular chaperone functions of heat-shock proteins. *Annual review of biochemistry*, *62*(1), 349-384.
54. Johnston, J. A., Ward, C. L., &Kopito, R. R. (1998). Aggresomes: a cellular response to misfolded proteins. *The Journal of cell biology*, *143*(7), 1883-1898.
55. Baneyx, F., &Mujacic, M. (2004). Recombinant protein folding and misfolding in Escherichia coli. *Nature biotechnology*, *22*(11), 1399-1408.
56. Mogk, A., Tomoyasu, T., Goloubinoff, P., Rüdiger, S., Röder, D., Langen, H., &Bukau, B. (1999). Identification of thermolabile Escherichia coli proteins: prevention and reversion of aggregation by DnaK and ClpB. *The EMBO journal*, *18*(24), 6934-6949.
57. Amarai, J. F., Marshalli, J., &Smithl, A. E. (1992). Processing of mutant cystic fibrosis transmembrane conductance regulator is temperature-sensitive. *nature*, *358*, 27.

58. Brown, C. R., Hong-Brown, L. Q., Biwersi, J., Verkman, A. S., & Welch, W. J. (1996). Chemical chaperones correct the mutant phenotype of the ΔF508 cystic fibrosis transmembrane conductance regulator protein. *Cell stress & chaperones*, *1*(2), 117.
59. Ghumman, B., Bertram, E. M., & Watts, T. H. (1998). Chemical chaperones enhance superantigen and conventional antigen presentation by HLA-DM-deficient as well as HLA-DM-sufficient antigen-presenting cells and enhance IgG2a production in vivo. *The Journal of Immunology*, *161*(7), 3262-3270.
60. Yang, D. S., Yip, C. M., Huang, T. J., Chakrabartty, A., & Fraser, P. E. (1999). Manipulating the amyloid-β aggregation pathway with chemical chaperones. *Journal of Biological Chemistry*, *274*(46), 32970-32974.
61. Yoshida, H., Yoshizawa, T., Shibasaki, F., Shoji, S. I., & Kanazawa, I. (2002). Chemical chaperones reduce aggregate formation and cell death caused by the truncated Machado–Joseph disease gene product with an expanded polyglutamine stretch. *Neurobiology of disease*, *10*(2), 88-99.
62. Perlmutter, D. H. (2002). Chemical chaperones: a pharmacological strategy for disorders of protein folding and trafficking. *Pediatric research*, *52*(6), 832-836.
63. Tatzelt, J., Prusiner, S. B., & Welch, W. J. (1996). Chemical chaperones interfere with the formation of scrapie prion protein. *The EMBO Journal*,*15*(23), 6363.
64. Pingarrón, J. M., Yañez-Sedeño, P., & González-Cortés, A. (2008). Gold nanoparticle-based electrochemical biosensors. *Electrochimica Acta*,*53*(19), 5848-5866.
65. Hainfeld, J. F., Slatkin, D. N., &Smilowitz, H. M. (2004). The use of gold nanoparticles to enhance radiotherapy in mice. *Physics in medicine and biology*, *49*(18), N309.
66. Lee, K. S., & El-Sayed, M. A. (2006). Gold and silver nanoparticles in sensing and imaging: sensitivity of plasmon response to size, shape, and metal composition. *The Journal of Physical Chemistry B*, *110*(39), 19220-19225.
67. J.Turkevich, P.C.Stevenson, J.Hiller (1951) A study of nucleation and growth processes in the synthesis of colloidal gold: *Discusss. Faraday soc.*1951, 11: 55-75
68. Majzik, A., Fülöp, L., Csapó, E., Bogár, F., Martinek, T., Penke, et al. (2010). Functionalization of gold nanoparticles with amino acid, β-amyloid peptides and fragment. *Colloids and Surfaces B: Biointerfaces*,*81*(1), 235-241.
69. Araya, E., Olmedo, I., Bastus, N. G., Guerrero, S., Puntes, V. F., Giralt, E., &Kogan, M. J. (2008). Gold nanoparticles and microwave irradiation inhibit beta-amyloid amyloidogenesis. *Nanoscale research letters*, *3*(11), 435-443.
70. Bellova, A., Bystrenova, E., Koneracka, M., Kopcansky, P., Valle, F., Tomasovicova, et al. (2010). Effect of Fe3O4 magnetic nanoparticles on lysozyme amyloid aggregation. *Nanotechnology*, *21*(6), 065103.
71. Liao, Y. H., Chang, Y. J., Yoshiike, Y., Chang, Y. C., & Chen, Y. R. (2012). Negatively Charged Gold Nanoparticles Inhibit Alzheimer's Amyloid-β Fibrillization, Induce Fibril Dissociation, and Mitigate Neurotoxicity. *Small*,*8*(23), 3631-3639.
72. Cabaleiro-Lago, C., Lynch, I., Dawson, K. A., &Linse, S. (2009). Inhibition of IAPP and IAPP (20− 29) fibrillation by polymeric nanoparticles.*Langmuir*, *26*(5), 3453-3461.
73. Porat, Y., Abramowitz, A., &Gazit, E. (2006). Inhibition of amyloid fibril formation by polyphenols: structural similarity and aromatic interactions as a common inhibition mechanism. *Chemical biology & drug design*,*67*(1), 27-
74. Lowe, T. L., Strzelec, A., Kiessling, L. L., & Murphy, R. M. (2001). Structure-function relationships for inhibitors of β-amyloid toxicity containing the recognition sequence KLVFF. *Biochemistry*, *40*(26), 7882-7889.

75. Watanabe, K. I., Nakamura, K., Akikusa, S., Okada, T., Kodaka, M., Konakahara, T., &Okuno, H. (2002). Inhibitors of fibril formation and cytotoxicity of β-amyloid peptide composed of KLVFF recognition element and flexible hydrophilic disrupting element. *Biochemical and biophysical research communications*, *290*(1), 121-124.
76. Moss, M. A., Nichols, M. R., Reed, D. K., Hoh, J. H., &Rosenberry, T. L. (2003). The peptide KLVFF-K6 promotes β-amyloid (1–40) protofibril growth by association but does not alter protofibril effects on cellular reduction of 3-(4, 5-dimethylthiazol-2-yl)-2, 5-diphenyltetrazolium bromide (MTT). *Molecular pharmacology*, *64*(5), 1160-1168.
77. Soto, C., Sigurdsson, E. M., Morelli, L., Kumar, R. A., Castaño, E. M., &Frangione, B. (1998). β-sheet breaker peptides inhibit fibrillogenesis in a rat brain model of amyloidosis: implications for Alzheimer's therapy.*Nature medicine*, *4*(7), 822-826.
78. Adessi, C., Frossard, M. J., Boissard, C., Fraga, S., Bieler, S., Ruckle, et al. (2003). Pharmacological profiles of peptide drug candidates for the treatment of Alzheimer's disease. *Journal of Biological chemistry*,*278*(16), 13905-13911.
79. Turner, J. P., Lutz-Rechtin, T., Moore, K. A., Rogers, L., Bhave, O., Moss, M. A., &Servoss, S. L. (2014). Rationally designed peptoids modulate aggregation of amyloid-beta 40. *ACS chemical neuroscience*, *5*(7), 552-558.
80. Moore, K., Wolf, L. M., Turner, J. P., Moss, M. A., &Servoss, S. (2015). The Effect of Peptoids on Aβ Aggregation and NF-κB Activation in Alzheimer's Disease. *Biophysical Journal*, *108*(2), 66a.
81. Biancalana, M.; Makabe, K.; Koide, A.; Koide, S. (2008) Molecular Mechanism of Thioflavin-T binding to the surface of β-rich peptide self-assemblies. Journal of molecular biology. 385: 1052-1063
82. Kayed, R., Head, E., Sarsoza, F., Saing, T., Cotman, C. W., Necula, et al. (2007). Fibril specific, conformation dependent antibodies recognize a generic epitope common to amyloid fibrils and fibrillar oligomers that is absent in prefibrillar oligomers. *MolNeurodegener*, *2*(18), 18.
83. Wu, W. H., Liu, Q., Sun, X., Yu, J. S., Zhao, D. S., Yu, Y. P., ... & Li, Y. M. (2013). Fibrillar seeds alleviate amyloid-β cytotoxicity by omitting formation of higher-molecular-weight oligomers. *Biochemical and biophysical research communications*, *439*(3), 321-326.
84. Ahmad, E., Ahmad, A., Singh, S., Arshad, M., Khan, A. H., & Khan, R. H. (2011). A mechanistic approach for islet amyloid polypeptide aggregation to develop anti-amyloidogenic agents for type-2 diabetes. *Biochimie*, *93*(5), 793-805.
85. Green, J. D., Goldsbury, C., Kistler, J., Cooper, G. J., &Aebi, U. (2004). Human amylin oligomer growth and fibril elongation define two distinct phases in amyloid formation. *Journal of Biological Chemistry*, *279*(13), 12206-12212.

A.2 List of Abbreviation

Aβ - Amyloid beta

AD - Alzheimer's disease

APP - Amyloid precursor protein

AuNP- Gold nano particle

CD - Circular dichroism

CFTR -Cystic fibrosis transmembrane conductance regulator

ER -Endoplasmic reticulum

Hsp - Heat shock protein

IAPP - Islet Amylin polypeptide

PCD- Protein conformational disorders

ThT- Thioflavin T

TEM - Transmission electron microscopy

A.3 List of Figures& Tables

Figure 1. Aβ protein to fibril development process

Figure 2. a) Aβ protein aggregation graph **b)** Aβ protein to fibril Development process

Figure 3. Peptide vs Peptoid structure

Figure 4. Gold nanoparticle synthesis

Figure 5. Structure of JPT1

Figure 6. Structure of JPT1s

Figure 7. Structure of JPT1a

Figure 8. Circular dichroism spectra of JPT1 and JPT1s.

Figure 9. ThT aggregation assay graph (control, JPT1, JPT1s, JPT1a)

Figure 10. Immunoblotting aggregation assay graph (control, JPT1, JPT1s, JPT1a)

Figure 11. TEM images of control (A: JPT1, B: JPT1s, C:JPT1a)

Figure 12. Similarity between human IAPP and amyloid beta protein.

Figure 13. Competition assay of aminated amylin- ThT binding with respect to JPT1

Figure 14. Competition assay of free acid amylin- ThT binding with respect to JPT1

Figure 15. ThT aggregation assay graph of aminated amylin with JPT1

Figure 16. ThT aggregation assay graph of free acid amylin with JPT1

Figure 17. TEM image for free acid amylin.
(A: Control Amylin, B: 40 μM of JPT1, C:100 μM of JPT1, D: 200 μM of JPT1)

Table 1. Summary of PCDs and their corresponding proteins

Figure 1: Tian, Y., Bassit, B., Chau, D., & Li, Y. M. (2010). An APP inhibitory domain containing the Flemish mutation residue modulates [gamma]-secretase activity for A [beta] production. *Nature structural & molecular biology*,*17*(2), 151-158.

Figure 2: Moore, K. A. (2013). Gold Nanoparticles and Peptoids as Novel Inhibitors of Amyloid Beta Aggregation in Alzheimer's Disease.

Figure3: CEM. (n.d.). Microwave Synthesis of Peptoids. Retrieved April 11, 2016, from http://www.cem.com/e107_files/public/pdf/bio-0012_mw_synthesis_of_peptoids.pdf

Figure4: Bahadur, K. C., Thapa, B., &Bhattarai, N. (2014). Gold nanoparticle-based gene delivery: promises and challenges. *Nanotechnology Reviews*, *3*(3), 269-280.

Figure 5-11: J..Phillips Turner, Dongwon Park, Melissa A. Moss, Shannon Servoss, Modulating Amyloid-& [beta] Aggregation: The Effects of Peptoid Side Chain Placement and Chirality (Submitted at Journal of Biological Chemistry in Sep2014)

Figure 12: Stefani, M., & Dobson, C. M. (2003). Protein aggregation and aggregate toxicity: new insights into protein folding, misfolding diseases and biological evolution. Journal of molecular medicine, 81(11), 678-699.

Figure 13-17: Tammy Lutz-Rechtin, Dongwon Park from Dr. Servoss' lab